HHS Public Access

Author manuscript

J Affect Disord. Author manuscript; available in PMC 2020 September 01.

Published in final edited form as:

J Affect Disord. 2019 September 01; 256: 33–41. doi:10.1016/j.jad.2019.05.067.

Treatment-Naïve First Episode Depression Classification Based on High-order Brain Functional Network

Yanting Zheng[1,2], **Xiaobo Chen**[2], **Danian Li**[3], **Yujie Liu**[1], **Xin Tan**[4], **Yi Liang**[4,2], **Han Zhang**[2,*], **Shijun Qiu**[4,*], **Dinggang Shen**[2,5,*]

[1]The First School of Clinical Medicine, Guangzhou University of Chinese Medicine, Guangzhou, Guangdong 510006, China

[2]Department of Radiology and BRIC, University of North Carolina at Chapel Hill, Chapel Hill, NC 27599, USA

[3]Cerebropathy Center, The First Affiliated Hospital of Guangzhou University of Chinese Medicine, Guangdong 510405, China

[4]Department of Radiology, The First Affiliated Hospital of Guangzhou University of Chinese Medicine, Guangdong 510405, China

[5]Department of Brain and Cognitive Engineering, Korea University, Seoul 02841, Republic of Korea

Abstract

Background: Recent functional connectivity (FC) studies have proved the potential value of resting-state functional magnetic resonance imaging (rs-fMRI) in the study of major depressive disorder (MDD); yet, the rs-fMRI-based individualized diagnosis of MDD is still challenging.

Methods: We enrolled 82 treatment-naïve first episode depression (FED) adults and 72 matched normal control (NC). A computer-aided diagnosis framework was utilized to classify the FEDs from the NCs based on the features extracted from not only traditional “low-order” FC networks (LON) based on temporal synchronization of original rs-fMRI signals, but also “high-order” FC networks (HON) that characterize more complex functional interactions via correlation of the dynamic (time-varying) FCs. We contrasted a classifier using HON feature (C_{HON}) and compared its performance with using LON only (C_{LON}). Finally, an integrated classification model with both features was proposed to further enhance FED classification.

*Corresponding Authors: Dinggang Shen, dgshen@med.unc.edu, +1-919-843-5420, 130 Mason Farm Road, Chapel Hill, NC 27599, USA, Han Zhang, hanzhang@med.unc.edu, +1-919-962-8135, 130 Mason Farm Road, Chapel Hill, NC 27599, USA, Shijun Qiu Shij_qiu@163.com, +86-20-36585090, 16 Jichang Road, Guangzhou 510405, China.

Contributors

Shijun Qiu, Han Zhang, Dinggang Shen designed the experiments. Yanting Zheng, Danian Li and Yujie Liu collected the data. Xiaobo Chen, Yanting Zheng and Yi Liang analyzed the data. Yanting Zheng, Xiaobo Chen, Han Zhang, Xin Tan wrote the paper. All the authors contributed to the interpretation of the results, manuscript revision, and have approved the final manuscript.

Conflicts of interest

The authors declare no conflict of interest.

Results: The C_{HON} had significantly improved diagnostic accuracy compared to the C_{LON} (82.47% vs. 67.53%). Joint classification further improved the performance (83.77%). The brain regions with potential diagnostic values mainly encompass the high-order cognitive function-related networks. Importantly, we found previously less-reported potential imaging biomarkers that involve the vermis and the crus II in the cerebellum.

Limitations: We only used one imaging modality and did not examine data from different subtypes of depression.

Conclusions: Depression classification could be significantly improved by using HON features that better capture the higher-level brain functional interactions. The findings suggest the importance of higher-level cerebro-cerebellar interactions in the pathophysiology of MDD.

Keywords

Depression; Treatment naïve; Functional magnetic resonance imaging; Dynamic functional connectivity

1. Introduction

Major depressive disorder (MDD) is the most common mental disease. It is characterized by the loss of interest or pleasure, a feeling of guilt and persistent sadness. According to the World Health Organization (WHO), over 300 million people are suffering from MDD worldwide, distinguishing this disorder among the ranks as the largest single contributor to disability (Geneva., 2017). The prevalence of MDD is close to 11–15% (Bromet et al., 2011) and the number of people living with MDD increased by 18.4% between 2005 and 2015 (Collaborators, 2016). However, the diagnosis of MDD is still challenging because the diagnosis is primarily based on both the patient's cooperation and the psychiatrist's experience (Kipli et al., 2013). It was also reported that primary care physicians with less experience could only correctly identify depression in about 50% of the positive case (Mitchell et al., 2009). The diagnosis could be complicated since the clinical signs may not always manifest. Due to the constraint of the number of experienced doctors, the length of consultation time, and the imbalance of medical resource, an accurate and objective method to help to diagnosis depression is in urgent need.

Magnetic resonance imaging (MRI) has been extensively used *in vivo* studies of MDD with different imaging modalities, such as structural MRI (Singh et al., 2013), functional MRI (fMRI) (Zhang et al., 2016), and diffusion tensor imaging (DTI) (Kieseppa et al., 2010). Machine learning methods have been utilized in studies of computer-aided MDD classification based on the image features from the non-invasive multimodal MRI (Orru et al., 2012). However, previous MRI-based MDD diagnosis studies have exhibited large variability in accuracy reported, which is ranging from 67.5% to 94.3% (Mwangi et al., 2012; Nouretdinov et al., 2011; Zeng et al., 2012). However, only a few imaging-based computer-aided MDD diagnosis studies have tackled treatment-naïve and first episode depression (FED). FED diagnosis is of more clinical value because a misdiagnosis may lead to unappropriated treatment causing prolonged illness duration and treatment resistance (Souery et al., 1999). Furthermore, previously applied antidepressant medicine could cause

alterations in brain function (Anand et al., 2005) and structures (Frodl et al., 2003), which could confound the computer-aided diagnosis. Taken together, the study of FED diagnosis could lead to a better understanding of depression-related pathological changes in the brain without possible interference by the confounding factors.

Due to the difficulty in FED subject enrollment, only handful studies had conducted MRI-based computer-aided treatment-naïve FED classification (Costafreda et al., 2009; Fang et al., 2012; Fu et al., 2008). A classification study focused on brain structural changes but reported unsatisfactory performance (Costafreda et al., 2009). Another paper used DTI-based structure connectivity for FED classification with high accuracy (Fang et al., 2012), but it was based on a limited sample size. Although a task-based fMRI study showed an increased FED diagnosis accuracy (Fu et al., 2008), the result may highly depend on the task and be affected by task-related confounding factors (e.g., different strategies and cooperation problem). In contrast to task-based fMRI, resting-state fMRI (rs-fMRI) does not require task performance. It is easy to implement in the clinical setting and places less demand on the patients. Therefore, rs-fMRI has been widely used in recent decades for disease studies. With the blood-oxygenation-level-depend (BOLD) signals measured for characterizing brain spontaneous activity (Cole et al., 2010), functional connectivity (FC) can be calculated on the temporal synchronization of the BOLD signals between any pair of brain regions. Previous studies have shown that FC is sensitive to various psychiatric diseases (Anderson et al., 2011; Shen et al., 2010), including depression (Greicius et al., 2007). To our best knowledge, only a few pioneering studies (Guo et al., 2012; Guo et al., 2014a) have used rs-fMRI to construct whole-brain FC networks for FED classification. However, their sample sizes are limited (N = 38 in (Guo et al., 2012) and N = 36 in (Guo et al., 2014a)), leading to concerns on the generalization ability (Arbabshirani et al., 2017). A relatively large sample size study of computer-aided FED diagnosis based on rs-fMRI and brain functional network is highly required.

In this study, we used a large group of treatment-naïve, FED patients to evaluate the feasibility of classification model and explore potential imaging biomarkers. Rather than only constructing simple FC networks based on the traditional pairwise temporal correlation of the BOLD signals (namely, "*low-order*" FC networks, or *LON*), we took a step further to construct a dynamic *"high-order" FC networks* (HON) to facilitate FED classification. The concept of the HON is based on our previous observations that temporal coherence among different time-resolved, dynamic FC links could be used as effective imaging markers in the detection of early Alzheimer's disease (Chen et al., 2016). In our following studies, we found that HON could reflect how the adaptive, state-related, time-varying FC are topologies are organized, which has been suggested to be more sensitive to disease-related changes than the conventional LON (Chen et al., 2017b; Zhang et al., 2017). In addition, HON could carry supplementary information to LON and jointly using both types of FC networks could further improve individual diagnosis (Liu et al., 2016).

In the present study, we proposed that HON characterize the more complex functional organization of the brain, which can help for FED diagnosis. Specifically, we aimed to construct classifiers by using HON with a relatively large sample of treatment-naïve FED rs-fMRI dataset and detect new imaging feature involving high-order cognitive function-related

brain areas. Collectively, we proposed a comprehensive rs-fMRI-based, automated FED classification model by fusing both HON and LON, which could be potentially applicable in the future studies on neurological and psychiatric diseases.

2. Methods

2.1 Participants

A total of 82 (53 females, 29 males) treatment-naïve FED adults and 72 (39 females, 33 males) age-, gender- and education-matched normal controls (NC) participated in this study from August 2015 to June 2017. The patients were recruited at The First Affiliated Hospital, Guangzhou University of Chinese Medicine, Guangdong, China. The diagnosis of treatment-naïve, first-episode depression was made between two attending psychiatrists who have more than 10 years of experience with Diagnostic and Statistical Manual of Mental Disorder (DSM-5) using the Structured Clinical Interview (SCID) (Qiu et al., 2018). A 17-item Hamilton Rating Scale for Depression (HAMD) (Hamilton, 1967) was used to evaluate depression severity (Guo et al., 2015). All the patients were at their first episode of depression and had no history of treatment, including antidepressants (e.g., antipsychotics, benzodiazepines or sedatives), psychotherapy and so on (Qiu et al., 2018). The inclusion criteria are: 1) aged between 18 and 55 years old, 2) right-handed native Chinese speaker, 3) no history of neurological illnesses or other psychiatric disorders (e.g., bipolar disorder, psychosis), and 4) HAMD ≥ 18. Subjects were excluded if they had significant systemic or neurologic illness, alcohol or drug abuse, or any contraindications to MRI scan. All NCs had HAMD-17 < 7. Two experienced radiologists determined that all subjects were normal on conventional MRI. Our inclusion criteria ensure that all our patients were treatment-naïve and at their first episode of depression (Qiu et al., 2018). All participants provided written informed consent and the study was approved by the Ethics Committee of the First Affiliated Hospital of Guangzhou University of Chinese Medicine, Guangzhou, China.

2.2 Data Acquisition and Preprocessing

In this work, MRI data were acquired with a 3.0T GE Singa HDxt scanner with 8-channel head coil. The conventional brain images included axial T1-weighted, T2-weighted, and fluid-attenuated inversion recovery (FLAIR) to exclude any cranial diseases. High-resolution T1-weighted images were acquired for registration purpose (repetition time (TR)/echo time (TE) = 10.4/4.3 ms, flip angle = 15°, slice thickness = 1.0 mm, slice gap = 0 mm, matrix size = 256 × 256, field of view (FOV) = 256 mm × 256 mm, and slices number = 156). The rs-fMRI parameters were: TR/TE = 2000/30 ms, flip angle = 90°, matrix size = 64 × 64, FOV = 240 mm × 240 mm, slices number = 33, slice thickness = 4.0 mm, scanning time = 8’20’’ (250 volumes). During the scan, subjects were instructed to remain still with their eyes closed and to avoid falling asleep. The rs-fMRI data were preprocessed by *DPARSF* version 2.3 (http://rfmri.org/DPARSF). Specifically, the first 10 volumes of each subject were discarded. After slice timing and head motion correction, T1 image was co-registered to the rs-fMRI from the same subject and further segmented using *unified segment* (http://www.fil.ion.ucl.ac.uk/spm) and registered to the standard Montreal Neurological Institute (MNI) space using *Diffeomorphic Anatomical Registration through Exponentiated Lie Algebra* (DARTEL). The rs-fMRI data was then warped to the MNI space, spatially

smoothed with a Gaussian kernel ($6 \times 6 \times 6$ mm^3), and temporally band-pass filtered (0.01−0.1Hz). After nuisance covariates regression, Automated Anatomical Labeling template (AAL) was applied to extract regional mean rs-fMRI time series of 116 regions-of-interest (ROIs). Subjects with maximum displacement in any directions larger than 2 mm or head rotation in any directions larger than 2° were excluded.

2.3 Classification based on High-order FC Networks

Our proposed classification framework based on HON is shown in Fig. 1. The steps of the training phase are as follows: 1) The entire BOLD signal were partitioned into multiple overlapping segments by using sliding windows, with window length set to 90 and the step size was 2 (Chen et al., 2016); 2) For each subject, a set of pair-wise LONs matrices were constructed from every BOLD signal segment, forming a dynamic FC time series for each link or ROI pair; 3) All subjects' dynamic FC time series were concatenated along the temporal dimension and then grouped into 800 clusters (Chen et al., 2017b); 4) By treating each cluster as a new node, a HON was constructed by calculating Pearson's correlation between each pair of cluster-averaged dynamic FC time series; 5) Weighted-graph-based local clustering coefficients (Rubinov and Sporns, 2010) were extracted for each node as a high-order FC feature (Jie et al., 2014); 6) A small subset of the informative high-order FC features were selected based on LASSO (Least Absolute Shrinkage and Selection Operator) (Tibshirani, 1996); and 7) a support vector machine (SVM) (Cortes and Vapnik, 1995) was learned based on the training subjects with the selected HON features. In the subsequent testing phase, the trained model was applied to the testing subjects and the performance of the classification on all the testing subjects was evaluated based on leave-one-out cross-validation (LOOCV). LOOCV can be essentially considered as a variant of k-fold (k = total number of subjects) cross-validation (Patel et al., 2016). Given L subjects, L-1 subjects are used for training, while the remaining one is used for testing in each loop of LOOCV. In this way, one can test the model established on the training set using the unseen subject. LOOCV is a popular, valid, and well-established method for testing a classification model in the field of machine learning (Wong, 2015). There are many other works also used LOOCV as the model evaluation method for testing the generalizability (Hahn et al., 2011; Mourao-Miranda et al., 2011), as when the samples are largely independent (like this study), the model has the lowest variability and without any bias to the mean accuracy (Bengio, 2004). Finally, the validation measures the average of values from all the iterations to evaluate the overall performance of our method. The details of the high-order FC and HON construction are detailed in our previous paper (Chen et al., 2016) and Supplementary Materials.

We compared the classification performance using HON only (C_{HON}) with that using traditional (static) LON only (C_{LON}) by repeating the above feature extraction, feature selection, and classification for LON. To jointly use the potentially complementary HON and LON features for even better FED classification, we trained two SVMs using LON and HON features, respectively. A combined classification was conducted by using an ensemble learning algorithm (Chen et al., 2017a), which integrates the two SVMs at the decision level by weighted linear combining the scores from them. This yielded a comprehensive FED identification model (i.e., $C_{HON+LON}$).

2.4 Identification of Discriminative Features

We ranked the HON (or LON) features based on the frequency during all cross-validation runs to figure out the discriminative features. We only chose the features that were 100% selected (indicating a good reproducibility). The values of these features were put into a subsequent regression analysis to further detect symptom-related features for both HON and LON.

2.5 Statistical Analysis

All the statistical analysis including demographic and clinical data were carried out using the SPSS version 23.0 (Chicago, IL, USA). Demographic and clinical data were compared between the two groups by using two-sample *t*-tests or chi-square tests. A p-value < 0.05 (two-tailed) was considered significant.

To investigate the association between multiple discriminative HON (or LON, for comparison) features and each of the two symptomatic variables (HAMD score and illness duration), a stepwise linear analysis (Song et al., 2008) was conducted for HON and LON, separately. The threshold was set as $p < 0.05$ (two-tailed). Age, gender, education level, the averaged strength of individual brain functional network, and the averaged clustering coefficients across all nodes were used as covariates during regression. The detailed procedure is provided in Supplementary Materials.

3. Results

3.1 Demographic and Clinical Data

The demographic and clinical information of the subject is summarized in Tab. 1. No significant difference was observed in gender, age, and education among FEDs and NCs.

3.2 High-order FC Network

Online Supplementary Fig. S1 shows the averaged connectivity matrices representing the group-level HON for two groups. For comparison, the results of the LON were shown. Visual comparison of the group averaged HONs shows greater differences between the FEDs and NCs (Online Supplementary Fig S1a, b), while such differences are less prominent with LONs (Online Supplementary Fig S1c, d).

3.3 HON-based FED *vs*. NC Classification

We evaluated the performances of the FED *vs*. NC classification using accuracy (ACC), area under curve (AUC) of the receiver operating characteristic (ROC) curve, sensitivity (SEN), specificity (SPE), Youden's Index (Youden), F-score, and balanced accuracy (BAC) (Sokolova et al., 2006). The equations of the indices are given in Supplementary Materials. The performance comparison results among $C_{HON,}$ $C_{LON,}$ and $C_{HON+LON}$ are shown in Tab. 2.

The proposed C_{HON} achieved much better results than C_{LON} with respect to all the performance indices. Specifically, the use of HONs boosted the FED classification accuracy by ~15% (to 82.47%), with balanced sensitivity (85.37%) and specificity (79.17%). In

contrast, LON led to less accurate (but still satisfactory considering the difficulty in separating the two groups) classification results. Moreover, $C_{HON+LON}$ achieved slightly better performance with an elevated AUC of ~0.91, which outperformed both C_{HON} and $C_{LON.}$ The ROC curves of the three methods are shown in Online Supplementary Fig. S2.

3.4 Discriminative HON Features

After discriminative feature identification, 28 HON features were consistently selected in all cross-validation runs and shown in Fig. 2. Most of the HON features had a star-shaped pattern with one hub region in the center, i.e., the cluster of the synchronized dynamic FC links shared one node (ROI). Many of these hub regions are located at the cerebellum, especially the vermis and the crus II. The other regions connected with the hubs are mainly located in the hippocampus, anterior cingulate gyrus (ACG), posterior cingulate gyrus (PCG), the orbitofrontal cortex (ORB), and the temporal pole. These regions mainly encompass the default mode network, central executive network, and salience network.

A total of 15 discriminative brain regions were consistently identified from the LON; they were visualized in Online Supplementary Fig. S3. These regions are mainly located at the hippocampus, PCG, temporal pole and cerebellum. Several of them are overlapped with the HON features as shown above, but they jointly achieved a lower FED classification accuracy.

3.5 Correlation between Imaging and Clinical Feature

Results from the stepwise linear regression are shown in Fig. 3 with multiple views of HON features and summarized in Online Supplementary Tab. S1. A total of four HON features (node #108, #265, #311 and #350) were found to be significantly correlated with the clinical scores. From the HON node #265, we found that several dynamic FC links that involve the thalamus and the cerebellar vermis are negatively associated with HAMD scores. The HON features with dynamic FC links encompassing ORB, inferior frontal gyrus (IFG) and temporal gyrus were associated with illness duration. Specifically, illness duration was negatively correlated with the HON node #311 and #350, including the dynamic FC clusters mainly involving cerebellum-to-cortex connections, where ORB, IFG, middle temporal gyrus (MTG) and inferior temporal gyrus (ITG) were involved. The positive correlation between depression duration and the HON feature is at HON node #108, which mainly encompasses cerebellum-to-subcortical regions, involving putamen (PUT) and pallidum (PAL). However, there is no significant correlation between the clinical scores and the LON features.

4. Discussion

In this study, we finally recruited 82 treatment-naïve FED patients and 72 normal controls. According to previous works, DSM-5 is used to diagnose depressive patients (Gong et al., 2018). Our stringent inclusion criteria and consensus-based diagnosis ensure that all the patients were at their first episode and treat-naïve (Qiu et al., 2018). However, it is not easy to make an accurate diagnosis of treatment-naïve first episode depression, especially for the primary care physicians with less experience. The diagnosis is challenging because it is

based on both the patient's cooperation and the psychiatrists' experience. Therefore, it is urgent to provide an accurate and objective method to help diagnose depression. In our study, we proposed an automated classification framework for individualized identification of treatment-naïve FED subjects, aiming to provide an effective model for helping identify treatment-naïve first episode major depressive disorder patients. Rs-fMRI is noninvasive and easy to perform during the clinical process. It can capture the sensitivity functional connectivity information between any paired regions of the brain, which may be regarded as promising biomarkers for early diagnosis of disease.

Instead of using traditional and static low-order FC, we calculated time-varying (dynamic) FC and further measured their temporal synchronization to model more complex higher-level functional associations. With HON, we improved the classification accuracy by 15% to 82%, thus further pushing boundaries of the clinically orientated rs-fMRI studies. In addition, we found that an ensemble of two types of functional networks further improved classification performance. The results indicate that the HON may serve as a feasible approach to study FED and, furthermore, the promising future of HON-based computer-aided clinical applications to help for diseases early diagnosis.

Of note, the feasibility of our method was tested with a relatively larger sample size of FEDs compared to the previous studies, together with rigorous cross-validation. Moreover, we revealed that the most discriminative brain regions were located at three major higher cognitive function-related "core networks" (Mulders et al., 2015), including the default mode network, central executive network, and salience network. Besides, we reported the significant role of the cerebellum in FED diagnosis, especially the vermis and the crus II. No LON but HON features within cerebellum-to-cortical/subcortical connections were found to be related to the clinical scores. The results indicate that higher-level cerebro-cerebellar connections can serve as potential image markers to distinguish FED.

4.1 Discriminative Brain Biomarkers in the "Core Networks"

We observed several discriminative brain regions for FED classification, including the hippocampus, ACG, PCG, ORB and the temporal pole, which are mainly within so-called "core networks". It contains the default mode network, salience network and central executive network, supporting higher cognitive functions in depression (Mulders et al., 2015). Among these regions, hippocampus, ACG, and PCG are involved in the default mode network (Laird et al., 2009) associated with depression (Guo et al., 2013; Guo et al., 2014b). The default mode network plays a key role in consciousness and memory processing in depression (Andrews-Hanna et al., 2014) and has a strong connection with the limbic system (Mulders et al., 2015). The limbic system, including the hippocampus and ACG, is believed to mediate emotion regulation and memory processing. The hippocampus mediates episodic memory, stress, negative emotion (Eichenbaum, 2013) and helplessness via gene expression (Kohen et al., 2005). The current finding of the hippocampus is consistent with the previous study (Shen et al., 2017) and is further supported by the animal model study, which suggested that glucocorticoid levels may negatively influence neurogenesis in the hippocampus (Campbell and MacQueen, 2004).

Our study revealed that ORB and the temporal pole, which are the components of the central executive network and salience network, respectively, could also be discriminative biomarkers for FED classification. The central executive network carries the function of attention regulation, working memory and decision-making (Miller and Cohen, 2001) while the salience network has a critical role in emotional control (Mulders et al., 2015). Previous studies explored the intrinsic relationship among three core networks in depression and found decreased FC between the default mode network and central executive network but increased between the default mode network and salience network (Manoliu et al., 2014). Our findings provide new evidence for the potential close relationship and possible complicated interactions among these core networks.

4.2 Vermis and Crus II in the Cerebellum

In this study, we found the cerebellum, especially the vermis and the crus II, connected with limbic/paralimbic, and orbitofrontal areas could be affected by depression. Fig. 2 showed that many hub regions are located at the cerebellum. Our findings not only further validated the previously believed higher-level cerebro-cerebellar interactions and their importance in maintaining normative psychological status but also provided new evidence of the impaired dynamic cerebral-cerebellum FCs in FED. Although the cerebellum is more related to motor coordination, researchers have found it has a close relationship with cognitive and emotion processing (Phillips et al., 2015). These observations are consistent with a few prior studies (Baldacara et al., 2008; Turner et al., 2007), showing a key role of the cerebellum in depression and its potential relationship with core networks. The sub-regions of the cerebellum were shown to be functionally coupled with the sensorimotor network and the cognitive control network in a human parcellation study (Buckner et al., 2011). Some of these connections are likely associated with depressive clinical symptoms such as slower movements and cognitive changes (Harvey et al., 2005). Meanwhile, animal experiments have explored the emotion regulative mechanism in the cerebellum. Cerebellar volume was positively correlated with social avoidance in mice (Anacker et al., 2016) and abnormal energy metabolism in amino acid metabolism, glycolysis, and adenosine triphosphate (ATP) biosynthesis were found in rat's cerebellum under chronic mild stress, a major risk factor for depression (Shao et al., 2015). An important contribution in this work is to demonstrate the dramatic influence of the cerebellum, providing new insight into the pathogenesis of MDD.

Our results also suggested that the vermis could be a potential biomarker for FED diagnosis. We observed that the connections between the vermis and the hippocampus, ORB as well as the thalamus, which are all believed to be critical in mood regulation (Bremner et al., 2002). The vermis, located in the midline of the cerebellum, has been found to mediate emotion and cognition (Schmahmann, 2004). In the early studies, researcher found notable behavioral and affective changes when the vermis had lesions (Schmahmann and Sherman, 1998). The abnormal structure and FC of the vermis have been found in a few depression studies. Yucel et al. found larger vermis volume in patients with MDD (Yucel et al., 2013), while a geriatric depression rs-fMRI study identified decreased FC of the left vermis with the ventromedial prefrontal cortex and PCG (Alalade et al., 2011). The vermis has putative connections to the limbic system (Schmahmann, 2000), which is also supported by animal studies (Vilensky and Vanhoesen, 1981). In addition, animal data also suggest direct connections between the

motor cortex and the vermis (Coffman et al., 2011), which may explain the movement symptom in depression. Collectively, our observation may indicate that vermis could be associated with depression symptoms via wide connections to the cortical and subcortical brain regions.

Alongside the vermis, the crus II may be another promising biomarker for FED diagnosis. Compared to the previous studies of the crus I about emotional processing (Krienen and Buckner, 2009) and working memory (Desmond et al., 1997) functions, not much attention has been paid to the crus II and its relationship with depression. A study of geriatric depression showed significantly reduced FC between the crus II and the ventromedial prefrontal cortex (Alalade et al., 2011). The cerebellum is believed to be coupled with cerebral association areas (e.g., default mode network), showing a possible role in memory and planning processing (Buckner et al., 2011). We observed that the connections between crus II and the precentral gyrus were correlated with the rating of depressive symptoms. We speculate such connections may indicate regulation of depression symptoms, providing the first evidence of the crus II's participation in the development of depression.

4.3 Correlation with Clinical Variables

In our study, the high-order FC between thalamus and the vermis were correlated with HAMD scores (Fig. 3a), while cerebellum, ORB, IFG, and temporal gyrus were correlated with illness duration (Fig. 3b–d). This result largely supplements the previous FED studies that found no significant correlation between the traditional static FC and the clinical scores (Wang et al., 2014; Zou et al., 2016). Specifically, a negative correlation was observed between the symptom severity and the local efficiency at the HON node #265, which involves synchronization dynamic FC between thalamus and the vermis. The more efficient this HON node is, the less severe depression the subject has. It is shown that the cerebellum has a widespread connection with the cerebral cortex (i.e., the cortico-cerebellum loop) via the thalamus (Heyder et al., 2004). Based on this, we further hypothesize that the more efficient vermis-to-thalamus high-order FC could make such a cerebro-cerebellar loop, thus either alleviating the depression symptom or being less affected by the depressive pathological attack.

Furthermore, the vermis and ORB were found to be negatively correlated with illness duration (Fig. 3b). That is, the more efficient these connections are, the shorter the time elapse to the commencement of the depression break. ORB is a part of the prefrontal cortex and it has been involved in decision making and expectation (Kringelbach, 2005). Furthermore, the prefrontal areas are responsible for negative emotional judgment in depression (Grimm et al., 2008). This result indicates that the cerebellum could link to the prefrontal cortex and such link could be weakened with the progression of the depression. Similar findings could be found at the HON node #350 (Fig. 3d), which are also cerebellum-to-cortex connections but involving widespread cerebral regions, including the ORB, IFG, and the temporal gyrus (MTG and ITG). This is in part accordance with previous MDD studies that showed similar negative correlations between illness duration and FC in the prefrontal gyrus and parietal cortex (Cao et al., 2012). In addition, IFG was suggested to be associated with emotion recognition (Shamay-Tsoory et al., 2009). A meta-analytic MDD

study also demonstrated that the temporal cortical regions active abnormally in response to positive emotional stimuli (Fitzgerald et al., 2008). MTG is located at the extended dorsal attention system and related to cued attention and working memory (Fox et al., 2006) and ITG is involved in high-level visual and memory processing (Freedman et al., 2003). Finally, illness duration had a positive correlation with the HON node #108 (Fig. 3c), involving cerebellum-to-subcortical (PUT and PAL) connections. PAL is related to emotion processing in depression (Diener et al., 2012). PUT is a key region in the hate circuit and associated with negative emotion stimuli in depression (Fitzgerald et al., 2008). The hate circuit is believed to process hate feeling and its abnormality might be associated with impaired cognitive control and cause over pervasive in the self-loathing, a common symptom in depression (Tao et al., 2013). A possible explanation of such a finding is that the high-order association between the cerebellum and PUT could be strengthened to attempt to control the abnormally processed negative emotions that could increase the disease prolonging.

4.4 Other issues

Since this is a machine learning-based classification study, the sample size becomes an important issue. Although our sample size (N = 154) was relatively large compared to the previous FED classification studies, it is still not large enough and we will have to increase the sample size in the future. Low statistical power and false positives may occur from small sample size in fMRI studies (Chen et al., 2018; Patel et al., 2016). A recent study reviewing 241 fMRI articles showed that the median sample size was 14.75 per group for two-group studies, resulting in unacceptable statistical power for most studies (Carp, 2012). Another study found that reliability, sensitivity and positive predictive value (PPV) rose steadily as the sample size increased (Chen et al., 2018). A recent study showed the prediction accuracy and its stability exponentially were found to increase with the increasing sample size, and the authors suggested a minimum sample size of 200 for machine learning regression prediction studies (Cui and Gong, 2018), based on which our sample size is acceptable. An interesting finding by a recent meta-analysis is reaffirming that “large samples are associated with narrower error margins and thus likely to tune classification results toward realistic estimates” (Neuhaus and Popescu, 2018). Especially for the machine learning-based depression diagnosis, the analysis found an inverse relationship between classification accuracy and sample size used in these classification studies and imaging modalities (Neuhaus and Popescu, 2018). The result can be further supported by a recent meta-analysis of multimodal MRI-based MDD diagnosis, where resting-state fMRI studies achieved better diagnostic sensitivity and specificity than structural MRI (Kambeitz et al., 2017).

It could be also beneficial if the FEDs can be separated into several symptom-based depression subtypes (melancholic, atypical and psychotic depression) or depression severity subgroups (mild depression, moderate depression, and severe depression), based on which the classification models can be trained to classify these subtypes or subgroups to unravel more meaningful findings. Depression severity is dynamically progressing and its diagnosis as mild depressed, moderate depressed, and severely depressed needs the evaluation by the experienced psychiatrist with DSM-5 using SCID. Previous research suggests that depression severity does not only rely on symptoms but also the degree of functional impartment, disability, or both (Park and Zarate, 2019), indicating that the symptom-based

subgrouping could actually be a much more complicated work than the case of merely using a 17-item Hamilton Rating Scale for Depression (HAMD). However, the aim of this study is to diagnose FEDs from normal controls, rather than diagnosing FED subgroups. A small sample size of different subgroups could negatively affect the model training and is more likely to cause an overfitting issue. Different depressive subtypes and severity subgroups could have different neurobiological mechanisms, and should be separately investigated with a larger sample size in the future.

There are several limitations to the study. First, we did not consider subgroups of depressive patients. Second, the current diagnostic model was only tested using LOOCV. On the other hand, *k*-fold cross-validation, another suitable cross-validation strategy for machine learning studies, can also be used to evaluate the model generalization ability, when provided adequate sample size. In the future, 80–20% (i.e., 5-fold) cross-validation could be adopted with a larger sample size to further test our model. Finally, we only used a single imaging modality and FC networks as features for classification. Other imaging modalities, such as diffusion tensor imaging (DTI), could provide supplementary (e.g., structural connectivity) diagnostic information and could be jointly used for better FED classification in the future.

4.5 Conclusions

In conclusions, based on large sample size, we, for the first time, construct a novel computer-aided individualized treatment-naïve FED classification model based on the resting-state dynamic FC and its spatiotemporal organization, high-order FC network (HON). We found that jointly using HON and LON achieve satisfactory accuracy in identification of FED individuals, showing the potential diagnostic value of the high-order FC between cerebellar and cerebral regions in mental disorder diagnosis. Our findings not only highlight the malfunctions of the core networks but also promising cerebellar biomarkers in depression.

Supplementary Material

Refer to Web version on PubMed Central for supplementary material.

Acknowledgement

Role of the funding source

Yanting Zheng, Yujie Liu, Xin Tan, Yi Liang, Shijun Qiu were partially supported by National Natural Science Foundation of China (91649117, 81771344, and 81471251), Shijun Qiu was also partially supported by Science and Technology Plan Project of Guangzhou (2018–1002-SF-0442) and Innovation and Strong School Project of Guangdong Provincial Education Department (2014GKXM034). Xiaobo Chen, Han Zhang, and Dinggang Shen were partially supported by an NIH grant (EB022880).

Abbreviations

FC	Functional connectivity
Rs-fMRI	Resting-state functional magnetic resonance imaging
FED	First episode depression

NC	Normal control
LON	Low-order FC networks
HON	High-order FC networks
MDD	Major depressive disorder
MRI	Magnetic resonance imaging
HAMD	Hamilton rating scale for depression
BOLD	Blood-oxygenation-level-depend

References

Alalade E, Denny K, Potter G, Steffens D, Wang LH, 2011 Altered Cerebellar-Cerebral Functional Connectivity in Geriatric Depression. PloS one 6 10.1371/journal.pone.0020035

Anacker C, Scholz J, O'Donnell KJ, Allemang-Grand R, Diorio J, Bagot RC, Nestler EJ, Hen R, Lerch JP, Meaney MJ, 2016 Neuroanatomic Differences Associated With Stress Susceptibility and Resilience. Biological psychiatry 79, 840–849. 10.1016/j.biopsych.2015.08.009 [PubMed: 26422005]

Anand A, Li Y, Wang Y, Wu J, Gao S, Bukhari L, Mathews VP, Kalnin A, Lowe MJ, 2005 Antidepressant effect on connectivity of the mood-regulating circuit: an FMRI study. Neuropsychopharmacology: official publication of the American College of Neuropsychopharmacology 30, 1334–1344. 10.1038/sj.npp.1300725 [PubMed: 15856081]

Anderson JS, Nielsen JA, Froehlich AL, DuBray MB, Druzgal TJ, Cariello AN, Cooperrider JR, Zielinski BA, Ravichandran C, Fletcher PT, Alexander AL, Bigler ED, Lange N, Lainhart JE, 2011 Functional connectivity magnetic resonance imaging classification of autism. Brain: a journal of neurology 134, 3742–3754. 10.1093/brain/awr263 [PubMed: 22006979]

Andrews-Hanna JR, Smallwood J, Spreng RN, 2014 The default network and self-generated thought: component processes, dynamic control, and clinical relevance. Ann Ny Acad Sci 1316, 29–52. 10.1093/brain/awr263 [PubMed: 24502540]

Arbabshirani MR, Plis S, Sui J, Calhoun VD, 2017 Single subject prediction of brain disorders in neuroimaging: Promises and pitfalls. NeuroImage 145, 137–165. 10.1016/j.neuroimage.2016.02.079 [PubMed: 27012503]

Baldacara L, Borgio JGF, de Lacerda ALT, Jackowski AP, 2008 Cerebellum and psychiatric disorders. Rev Bras Psiquiatr 30, 281–289. 10.1590/S1516-44462008000300016 [PubMed: 18833430]

Bengio Y, 2004 No Unbiased Estimator of the Variance of K-Fold Cross-Validation. Journal of Machine Learning Research 5, 1089–1105. http://www.jmlr.org/papers/v5/grandvalet04a.html?92f58540

Bremner JD, Vythilingam M, Vermetten E, Nazeer A, Adil J, Khan S, Staib LH, Charney DS, 2002 Reduced volume of orbitofrontal cortex in major depression. Biological psychiatry 51, 273–279. 10.1016/S0006-3223(01)01336-1 [PubMed: 11958777]

Bromet E, Andrade LH, Hwang I, Sampson NA, Alonso J, de Girolamo G, de Graaf R, Demyttenaere K, Hu C, Iwata N, Karam AN, Kaur J, Kostyuchenko S, Lepine JP, Levinson D, Matschinger H, Mora ME, Browne MO, Posada-Villa J, Viana MC, Williams DR, Kessler RC, 2011 Cross-national epidemiology of DSM-IV major depressive episode. BMC medicine 9, 90 10.1186/1741-7015-9-90 [PubMed: 21791035]

Buckner RL, Krienen FM, Castellanos A, Diaz JC, Yeo BT, 2011 The organization of the human cerebellum estimated by intrinsic functional connectivity. Journal of neurophysiology 106, 2322–2345. 10.1152/jn.00339.2011 [PubMed: 21795627]

Campbell S, MacQueen G, 2004 The role of the hippocampus in the pathophysiology of major depression. J Psychiatr Neurosci 29, 417–426. 10.1037/t01554-000

Cao X, Liu Z, Xu C, Li J, Gao Q, Sun N, Xu Y, Ren Y, Yang C, Zhang K, 2012 Disrupted resting-state functional connectivity of the hippocampus in medication-naive patients with major depressive disorder. Journal of affective disorders 141, 194–203. 10.1016/j.jad.2012.03.002 [PubMed: 22460056]

Carp J, 2012 The secret lives of experiments: methods reporting in the fMRI literature. NeuroImage 63, 289–300. http://www.ncbi.nlm.nih.gov/pubmed/22796459 [PubMed: 22796459]

Chen X, Lu B, Yan CG, 2018 Reproducibility of R-fMRI metrics on the impact of different strategies for multiple comparison correction and sample sizes. Human brain mapping 39, 300–318. http://www.ncbi.nlm.nih.gov/pubmed/29024299 [PubMed: 29024299]

Chen X, Zhang H, Gao Y, Wee CY, Li G, Shen D, Alzheimer's Disease Neuroimaging, I., 2016 High-order resting-state functional connectivity network for MCI classification. Human brain mapping 37, 3282–3296. 10.1002/hbm.23240 [PubMed: 27144538]

Chen X, Zhang H, Zhang L, Shen C, Lee SW, Shen D, 2017a Extraction of dynamic functional connectivity from brain grey matter and white matter for MCI classification. Human brain mapping 38, 5019–5034. 10.1002/hbm.23711 [PubMed: 28665045]

Chen XB, Zhang H, Lee SW, Shen DG, Neuroimaging, A.s.D., 2017b Hierarchical High-Order Functional Connectivity Networks and Selective Feature Fusion for MCI Classification. Neuroinformatics 15, 271–284. 10.1007/s12021-017-9330-4 [PubMed: 28555371]

Coffman KA, Dum RP, Strick PL, 2011 Cerebellar vermis is a target of projections from the motor areas in the cerebral cortex. P Natl Acad Sci USA 108, 16068–16073. 10.1073/pnas.1107904108

Cole DM, Smith SM, Beckmann CF, 2010 Advances and pitfalls in the analysis and interpretation of resting-state FMRI data. Frontiers in systems neuroscience 4, 8 10.3389/fnsys.2010.00008 eCollection2010 [PubMed: 20407579]

Collaborators, G.D.a.I.I.a.P., 2016 Global, regional, and national incidence, prevalence, and years lived with disability for 310 diseases and injuries, 1990–2015: a systematic analysis for the Global Burden of Disease Study 2015. Lancet 388, 1545–1602. 10.1016/S0140-6736(16)31678-6 [PubMed: 27733282]

Cortes C, Vapnik V, 1995 Support-Vector Networks. Mach Learn 20, 273–297. 10.1007/BF00994018

Costafreda SG, Chu C, Ashburner J, Fu CH, 2009 Prognostic and diagnostic potential of the structural neuroanatomy of depression. PloS one 4, e6353 10.1371/journal.pone.0006353 [PubMed: 19633718]

Cui Z, Gong G, 2018 The effect of machine learning regression algorithms and sample size on individualized behavioral prediction with functional connectivity features. NeuroImage 178, 622–637. 10.1016/j.neuroimage.2018.06.001 [PubMed: 29870817]

Desmond JE, Gabrieli JDE, Wagner AD, Ginier BL, Glover GH, 1997 Lobular patterns of cerebellar activation in verbal working-memory and finger-tapping tasks as revealed by functional MRI. Journal of Neuroscience 17, 9675–9685. 10.1523/JNEUROSCI.17-24-09675.1997 [PubMed: 9391022]

Diener C, Kuehner C, Brusniak W, Ubl B, Wessa M, Flor H, 2012 A meta-analysis of neurofunctional imaging studies of emotion and cognition in major depression. NeuroImage 61, 677–685. 10.1016/j.neuroimage.2012.04.005 [PubMed: 22521254]

Eichenbaum H, 2013 Hippocampus: Remembering the Choices. Neuron 77, 999–1001. 10.1016/j.neuron.2013.02.034 [PubMed: 23522037]

Fang P, Zeng LL, Shen H, Wang L, Li B, Liu L, Hu D, 2012 Increased cortical-limbic anatomical network connectivity in major depression revealed by diffusion tensor imaging. PloS one 7, e45972 10.1371/journal.pone.0045972 [PubMed: 23049910]

Fitzgerald PB, Laird AR, Maller J, Daskalakis ZJ, 2008 A meta-analytic study of changes in brain activation in depression. Human brain mapping 29, 683–695. 10.1002/hbm.20426 [PubMed: 17598168]

Fox MD, Corbetta M, Snyder AZ, Vincent JL, Raichle ME, 2006 Spontaneous neuronal activity distinguishes human dorsal and ventral attention systems. Proceedings of the National Academy of Sciences of the United States of America 103, 13560–13560. 10.1073/pnas.0604187103

Freedman DJ, Riesenhuber M, Poggio T, Miller EK, 2003 A comparison of primate prefrontal and inferior temporal cortices during visual categorization. J Neurosci 23, 5235–5246. 10.1523/JNEUROSCI.23-12-05235.2003 [PubMed: 12832548]

Frodl T, Meisenzahl EM, Zetzsche T, Born C, Jager M, Groll C, Bottlender R, Leinsinger G, Moller HJ, 2003 Larger amygdala volumes in first depressive episode as compared to recurrent major depression and healthy control subjects. Biological psychiatry 53, 338–344. 10.1016/S0006-3223(02)01474-9 [PubMed: 12586453]

Fu CH, Mourao-Miranda J, Costafreda SG, Khanna A, Marquand AF, Williams SC, Brammer MJ, 2008 Pattern classification of sad facial processing: toward the development of neurobiological markers in depression. Biological psychiatry 63, 656–662. 10.1016/j.biopsych.2007.08.020 [PubMed: 17949689]

Geneva., 2017 Depression and other common mental disorders: Global health estimates World Health Organization https://www.who.int/mental_health/management/depression/prevalence_global_health_estimates/en/

Gong L, Hou Z, Wang Z, He C, Yin Y, Yuan Y, Zhang H, Lv L, Zhang H, Xie C, Zhang Z, 2018 Disrupted topology of hippocampal connectivity is associated with short-term antidepressant response in major depressive disorder. Journal of affective disorders 225, 539–544. http://www.ncbi.nlm.nih.gov/pubmed/28866298 [PubMed: 28866298]

Greicius MD, Flores BH, Menon V, Glover GH, Solvason HB, Kenna H, Reiss AL, Schatzberg AF, 2007 Resting-state functional connectivity in major depression: Abnormally increased contributions from subgenual cingulate cortex and thalamus. Biological psychiatry 62, 429–437. 10.1016/j.biopsych.2006.09.020 [PubMed: 17210143]

Grimm S, Beck J, Schuepbach D, Hell D, Boesiger P, Bermpohl F, Niehaus L, Boeker H, Northoff G, 2008 Imbalance between left and right dorsolateral prefrontal cortex in major depression is linked to negative emotional judgment: An fMRI study in severe major depressive disorder. Biological psychiatry 63, 369–376. 10.1016/j.biopsych.2007.05.033 [PubMed: 17888408]

Guo H, Cao X, Liu Z, Li H, Chen J, Zhang K, 2012 Machine learning classifier using abnormal brain network topological metrics in major depressive disorder. Neuroreport 23, 1006–1011. 10.1097/WNR.0b013e32835a650c [PubMed: 23044496]

Guo H, Cheng C, Cao XH, Xiang J, Chen JJ, Zhang KR, 2014a Resting-state functional connectivity abnormalities in first-onset unmedicated depression. Neural Regen Res 9, 153–163. 10.4103/1673-5374.125344 [PubMed: 25206796]

Guo W, Liu F, Dai Y, Jiang M, Zhang J, Yu L, Long L, Chen H, Gao Q, Xiao C, 2013 Decreased interhemispheric resting-state functional connectivity in first-episode, drug-naive major depressive disorder. Progress in neuro-psychopharmacology & biological psychiatry 41, 24–29. 10.1016/j.pnpbp.2012.11.003 [PubMed: 23159796]

Guo W, Liu F, Xiao C, Zhang Z, Liu J, Yu M, Zhang J, Zhao J, 2015 Decreased insular connectivity in drug-naive major depressive disorder at rest. Journal of affective disorders 179, 31–37. http://www.ncbi.nlm.nih.gov/pubmed/25845747 [PubMed: 25845747]

Guo W, Liu F, Zhang J, Zhang Z, Yu L, Liu J, Chen H, Xiao C, 2014b Abnormal default-mode network homogeneity in first-episode, drug-naive major depressive disorder. PloS one 9, e91102 10.1371/journal.pone.0091102 [PubMed: 24609111]

Hahn T, Marquand AF, Ehlis AC, Dresler T, Kittel-Schneider S, Jarczok TA, Lesch KP, Jakob PM, Mourao-Miranda J, Brammer MJ, Fallgatter AJ, 2011 Integrating neurobiological markers of depression. Archives of general psychiatry 68, 361–368. http://www.ncbi.nlm.nih.gov/pubmed/21135315 [PubMed: 21135315]

Hamilton M, 1967 Development of a Rating Scale for Primary Depressive Illness. Brit J Soc Clin Psyc 6, 278–96. 10.1111/j.2044-8260.1967.tb00530.x

Harvey PO, Fossati P, Pochon JB, Levy R, LeBastard G, Lehericy S, Allilaire JF, Dubois B, 2005 Cognitive control and brain resources in major depression: An fMRI study using the n-back task. NeuroImage 26, 860–869. 10.1016/j.neuroimage.2005.02.048 [PubMed: 15955496]

Heyder K, Suchan B, Daum I, 2004 Cortico-subcortical contributions to executive control. Acta Psychol 115, 271–289. 10.1016/j.actpsy.2003.12.010

Jie B, Zhang DQ, Gao W, Wang Q, Wee CY, Shen DG, 2014 Integration of Network Topological and Connectivity Properties for Neuroimaging Classification. Ieee T Bio-Med Eng 61, 576–589. 10.1109/TBME.2013.2284195

Kambeitz J, Cabral C, Sacchet MD, Gotlib IH, Zahn R, Serpa MH, Walter M, Falkai P, Koutsouleris N, 2017 Detecting Neuroimaging Biomarkers for Depression: A Meta-analysis of Multivariate Pattern Recognition Studies. Biological psychiatry 82, 330–338. http://www.ncbi.nlm.nih.gov/pubmed/28110823 [PubMed: 28110823]

Kieseppa T, Eerola M, Mantyla R, Neuvonen T, Poutanen VP, Luoma K, Tuulio-Henriksson A, Jylha P, Mantere O, Melartin T, Rytsala H, Vuorilehto M, Isometsa E, 2010 Major depressive disorder and white matter abnormalities: A diffusion tensor imaging study with tract-based spatial statistics. Journal of affective disorders 120, 240–244. 10.1016/j.jad.2009.04.023 [PubMed: 19467559]

Kipli K, Kouzani AZ, Williams LJ, 2013 Towards automated detection of depression from brain structural magnetic resonance images. Neuroradiology 55, 567–584. 10.1007/s00234-013-1139-8 [PubMed: 23338839]

Kohen R, Kirov S, Navaja GP, Happe HK, Hamblin MW, Snoddy JR, Neumaier JF, Petty F, 2005 Gene expression profiling in the hippocampus of learned helpless and nonhelpless rats. Pharmacogenomics J 5, 278–291. 10.1038/sj.tpj.6500322 [PubMed: 16010284]

Krienen FM, Buckner RL, 2009 Segregated Fronto-Cerebellar Circuits Revealed by Intrinsic Functional Connectivity. Cerebral cortex 19, 2485–2497. 10.1093/cercor/bhp135 [PubMed: 19592571]

Kringelbach ML, 2005 The human orbitofrontal cortex: linking reward to hedonic experience. Nature Reviews Neuroscience 6, 691 10.1038/nrn1747 [PubMed: 16136173]

Laird AR, Eickhoff SB, Li K, Robin DA, Glahn DC, Fox PT, 2009 Investigating the functional heterogeneity of the default mode network using coordinate-based meta-analytic modeling. The Journal of neuroscience : the official journal of the Society for Neuroscience 29, 14496–14505. 10.1523/JNEUROSCI.4004-09.2009 [PubMed: 19923283]

Liu L, Zhang H, Rekik I, Chen X, Wang Q, Shen D, 2016 Outcome Prediction for Patient with High-Grade Gliomas from Brain Functional and Structural Networks. Medical image computing and computer-assisted intervention : MICCAI … International Conference on Medical Image Computing and Computer-Assisted Intervention 9901, 26–34. 10.1007/978-3-319-46723-8_4

Manoliu A, Meng C, Brandl F, Doll A, Tahmasian M, Scherr M, Schwerthoffer D, Zimmer C, Forstl H, Bauml J, Riedl V, Wohlschlager AM, Sorg C, 2014 Insular dysfunction within the salience network is associated with severity of symptoms and aberrant inter-network connectivity in major depressive disorder. Frontiers in human neuroscience 7 10.3389/fnhum.2013.00930. eCollection 2013

Miller EK, Cohen JD, 2001 An integrative theory of prefrontal cortex function. Annu Rev Neurosci 24, 167–202. 10.1146/annurev.neuro.24.1.167 [PubMed: 11283309]

Mitchell AJ, Vaze A, Rao S, 2009 Clinical diagnosis of depression in primary care: a meta-analysis. Lancet 374, 609–619. 10.1016/S0140-6736(09)60879-5 [PubMed: 19640579]

Mourao-Miranda J, Hardoon DR, Hahn T, Marquand AF, Williams SC, Shawe-Taylor J, Brammer M, 2011 Patient classification as an outlier detection problem: an application of the One-Class Support Vector Machine. NeuroImage 58, 793–804. 10.1016/j.neuroimage.2011.06.042 [PubMed: 21723950]

Mulders PC, van Eijndhoven PF, Schene AH, Beckmann CF, Tendolkar I, 2015 Resting-state functional connectivity in major depressive disorder: A review. Neuroscience and biobehavioral reviews 56, 330–344. 10.1016/j.neubiorev.2015.07.014 [PubMed: 26234819]

Mwangi B, Ebmeier KP, Matthews K, Steele JD, 2012 Multi-centre diagnostic classification of individual structural neuroimaging scans from patients with major depressive disorder. Brain : a journal of neurology 135, 1508–1521. 10.1093/brain/aws084 [PubMed: 22544901]

Neuhaus AH, Popescu FC, 2018 Sample Size, Model Robustness, and Classification Accuracy in Diagnostic Multivariate Neuroimaging Analyses. Biological psychiatry 84, e81–e82. 10.1016/j.biopsych.2017.09.032 [PubMed: 29580571]

Nouretdinov I, Costafreda SG, Gammerman A, Chervonenkis A, Vovk V, Vapnik V, Fu CH, 2011 Machine learning classification with confidence: application of transductive conformal predictors

to MRI-based diagnostic and prognostic markers in depression. NeuroImage 56, 809–813. 10.1016/j.neuroimage.2010.05.023 [PubMed: 20483379]

Orru G, Pettersson-Yeo W, Marquand AF, Sartori G, Mechelli A, 2012 Using Support Vector Machine to identify imaging biomarkers of neurological and psychiatric disease: a critical review. Neuroscience and biobehavioral reviews 36, 1140–1152. 10.1016/j.neubiorev.2012.01.004 [PubMed: 22305994]

Park LT, Zarate CA Jr., 2019 Depression in the Primary Care Setting. The New England journal of medicine 380, 559–568. http://www.ncbi.nlm.nih.gov/pubmed/30726688 [PubMed: 30726688]

Patel MJ, Khalaf A, Aizenstein HJ, 2016 Studying depression using imaging and machine learning methods. NeuroImage. Clinical 10, 115–123. http://www.ncbi.nlm.nih.gov/pubmed/26759786 [PubMed: 26759786]

Phillips JR, Hewedi DH, Eissa AM, Moustafa AA, 2015 The cerebellum and psychiatric disorders. Frontiers in public health 3, 66 10.3389/fpubh.2015.00066 [PubMed: 26000269]

Qiu L, Xia M, Cheng B, Yuan L, Kuang W, Bi F, Ai H, Gu Z, Lui S, Huang X, He Y, Gong Q, 2018 Abnormal dynamic functional connectivity of amygdalar subregions in untreated patients with first-episode major depressive disorder. Journal of Psychiatry Neuroscience 43, 262–272. https://www.ncbi.nlm.nih.gov/pmc/articles/PMC6019355/ [PubMed: 29947609]

Rubinov M, Sporns O, 2010 Complex network measures of brain connectivity: Uses and interpretations. Neuroimage 52, 1059–1069. 10.1016/j.neuroimage.2009.10.003 [PubMed: 19819337]

Schmahmann JD, 2000 The role of the cerebellum in affect and psychosis. J Neurolinguist 13, 189–214. 10.1016/S0911-6044(00)00011-7

Schmahmann JD, 2004 Disorders of the cerebellum: Ataxia, dysmetria of thought, and the cerebellar cognitive affective syndrome. J Neuropsych Clin N 16, 367–378. 10.1176/jnp.16.3.367

Schmahmann JD, Sherman JC, 1998 The cerebellar cognitive affective syndrome. Brain : a journal of neurology 121, 561–579. 10.1093/brain/121.4.561 [PubMed: 9577385]

Shamay-Tsoory SG, Aharon-Peretz J, Perry D, 2009 Two systems for empathy: a double dissociation between emotional and cognitive empathy in inferior frontal gyrus versus ventromedial prefrontal lesions. Brain 132, 617–627. 10.1093/brain/awn279 [PubMed: 18971202]

Shao WH, Chen JJ, Fan SH, Lei Y, Xu HB, Zhou J, Cheng PF, Yang YT, Rao CL, Wu B, Liu HP, Xie P, 2015 Combined Metabolomics and Proteomics Analysis of Major Depression in an Animal Model: Perturbed Energy Metabolism in the Chronic Mild Stressed Rat Cerebellum. Omics: a journal of integrative biology 19, 383–392. 10.1089/omi.2014.0164 [PubMed: 26134254]

Shen H, Wang LB, Liu YD, Hu DW, 2010 Discriminative analysis of resting-state functional connectivity patterns of schizophrenia using low dimensional embedding of fMRI. NeuroImage 49, 3110–3121. 10.1016/j.neuroimage.2009.11.011 [PubMed: 19931396]

Shen ZL, Jiang LL, Yang SR, Ye J, Dai N, Liu XY, Li N, Lu J, Liu F, Lu Y, Sun XJ, Cheng YQ, Xu XF, 2017 Identify changes of brain regional homogeneity in early and later adult onset patients with first-episode depression using resting-state fMRI. PloS one 12 10.1371/journal.pone.0184712

Singh MK, Kesler SR, Hosseini SMH, Kelley RG, Amatya D, Hamilton JP, Chen MC, Gotlib IH, 2013 Anomalous Gray Matter Structural Networks in Major Depressive Disorder. Biological psychiatry 74, 777–785. 10.1016/j.biopsych.2013.03.005 [PubMed: 23601854]

Sokolova M, Japkowicz N, Szpakowicz S, 2006 Beyond accuracy, F-score and ROC: a family of discriminant measures for performance evaluation, Australasian joint conference on artificial intelligence Springer, pp. 1015–1021. 10.1007/11941439_114

Song M, Zhou Y, Li J, Liu Y, Tian L, Yu C, Jiang T, 2008 Brain spontaneous functional connectivity and intelligence. NeuroImage 41, 1168–1176. 10.1016/j.neuroimage.2008.02.036 [PubMed: 18434203]

Souery D, Amsterdam J, de Montigny C, Lecrubier Y, Montgomery S, Lipp O, Racagni G, Zohar J, Mendlewicz J, 1999 Treatment resistant depression: methodological overview and operational criteria. Eur Neuropsychopharm 9, 83–91. 10.1016/S0924-977X(98)00004-2

Tao H, Guo S, Ge T, Kendrick KM, Xue Z, Liu Z, Feng J, 2013 Depression uncouples brain hate circuit. Molecular psychiatry 18, 101–111. 10.1038/mp.2011.127. Epub 2011 Oct 4 [PubMed: 21968929]

Tibshirani R, 1996 Regression shrinkage and selection via the Lasso. J Roy Stat Soc B Met 58, 267–288. 10.1111/j.2517-6161.1996.tb02080.x

Turner BM, Paradiso S, Marvel CL, Pierson R, Ponto LLB, Hichwa RD, Robinson RG, 2007 The cerebellum and emotional experience. Neuropsychologia 45, 1331–1341. 10.1016/j.neuropsychologia.2006.09.023 [PubMed: 17123557]

Vilensky JA, Vanhoesen GW, 1981 Corticopontine Projections from the Cingulate Cortex in the Rhesus-Monkey. Brain research 205, 391–395. 10.1016/0006-8993(81)90348-6 [PubMed: 7470872]

Wang L, Li K, Zhang Q, Zeng Y, Dai W, Su Y, Wang G, Tan Y, Jin Z, Yu X, Si T, 2014 Short-term effects of escitalopram on regional brain function in first-episode drug-naive patients with major depressive disorder assessed by resting-state functional magnetic resonance imaging. Psychological medicine 44, 1417–1426. 10.1017/S0033291713002031 [PubMed: 23942213]

Wong T-T, 2015 Performance evaluation of classification algorithms by k-fold and leave-one-out cross validation. Pattern Recognition 48, 2839–2846. 10.1016/j.patcog.2015.03.009

Yucel K, Nazarov A, Taylor VH, Macdonald K, Hall GB, MacQueen GM, 2013 Cerebellar vermis volume in major depressive disorder. Brain Structure and Function 218, 851–858. 10.1007/s00429-012-0433-2 [PubMed: 22696069]

Zeng LL, Shen H, Liu L, Wang L, Li B, Fang P, Zhou Z, Li Y, Hu D, 2012 Identifying major depression using whole-brain functional connectivity: a multivariate pattern analysis. Brain : a journal of neurology 135, 1498–1507. 10.1093/brain/aws059 [PubMed: 22418737]

Zhang H, Chen X, Zhang Y, Shen D, 2017 Test-Retest Reliability of “High-Order” Functional Connectivity in Young Healthy Adults. Frontiers in neuroscience 11, 439 10.3389/fnins.2017.00439 [PubMed: 28824362]

Zhang X, Di X, Lei H, Yang J, Xiao J, Wang X, Yao S, Rao H, 2016 Imbalanced spontaneous brain activity in orbitofrontal-insular circuits in individuals with cognitive vulnerability to depression. Journal of affective disorders 198, 56–63. 10.1016/j.jad.2016.03.001 [PubMed: 27011360]

Zou K, Gao Q, Long Z, Xu F, Sun X, Chen H, Sun X, 2016 Abnormal functional connectivity density in first-episode, drug-naive adult patients with major depressive disorder. Journal of affective disorders 194, 153–158. 10.1016/j.jad.2015.12.081 [PubMed: 26826535]

Highlights:

- High-order functional connectivity networks can capture dynamic and higher-level brain functional interactions, indicating potential value for treatment-naïve, first episode depression diagnosis.
- The default mode network, central executive network and salience network are regarded as three major higher cognitive function-related “core networks” in treatment-naïve, first episode depression.
- The high-level interactions between cerebellar and cerebral regions could be the key neuroimaging indications in depression.

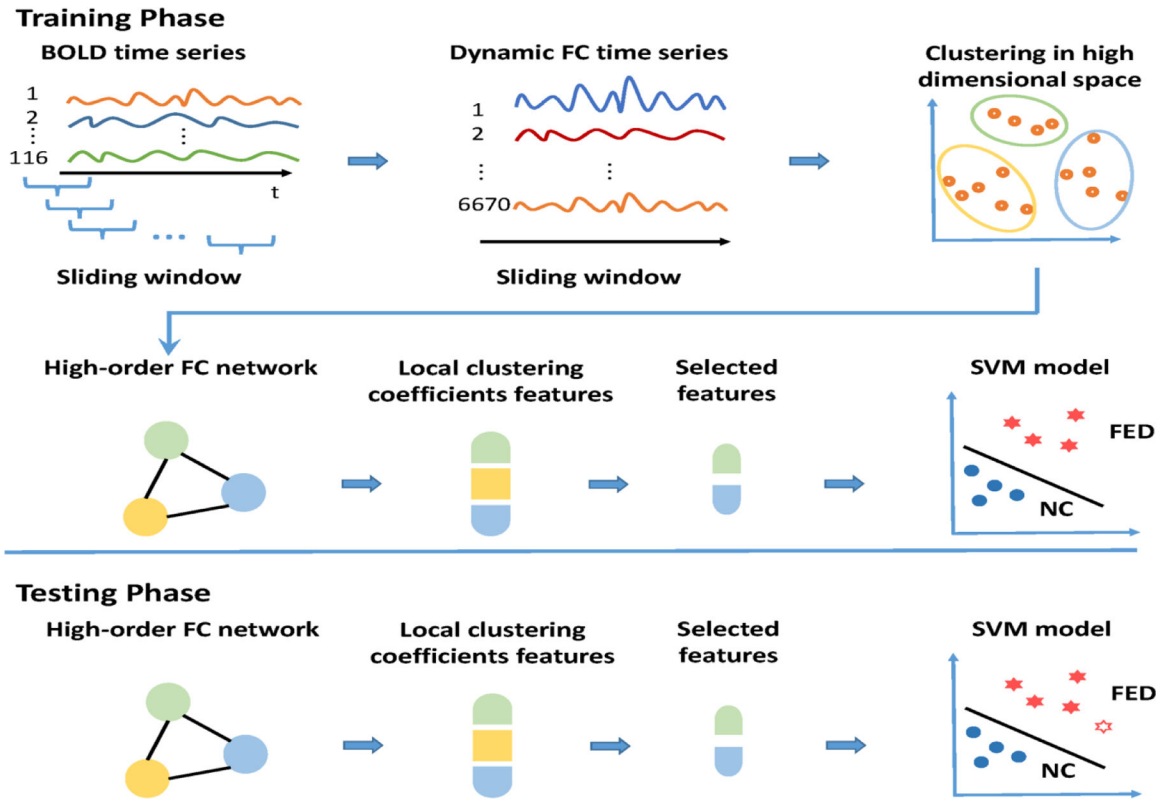

Fig. 1. Framework for FED classification based on the high-order FC network (HON).

Both the training phase (top) and testing phase (bottom) are shown. The training phase includes sliding window-based dynamic FC analysis for all the 6670 pairs of brain regions (a total of 116 ROIs based on AAL template), clustering the dynamic FC time series of all subjects. HON construction was based on correlation analysis of the cluster-wise dynamic FC time series. After HON features extraction and selection, a support vector machine (SVM)-based classification was used. In the testing phase, the re-fMRI data of new subjects went through the entire processing and the trained classification model until the diagnosis performance was generated.

Abbreviations: BOLD, blood oxygenation level-depend; FC, functional connectivity; FED, first episode depression; NC, normal control.

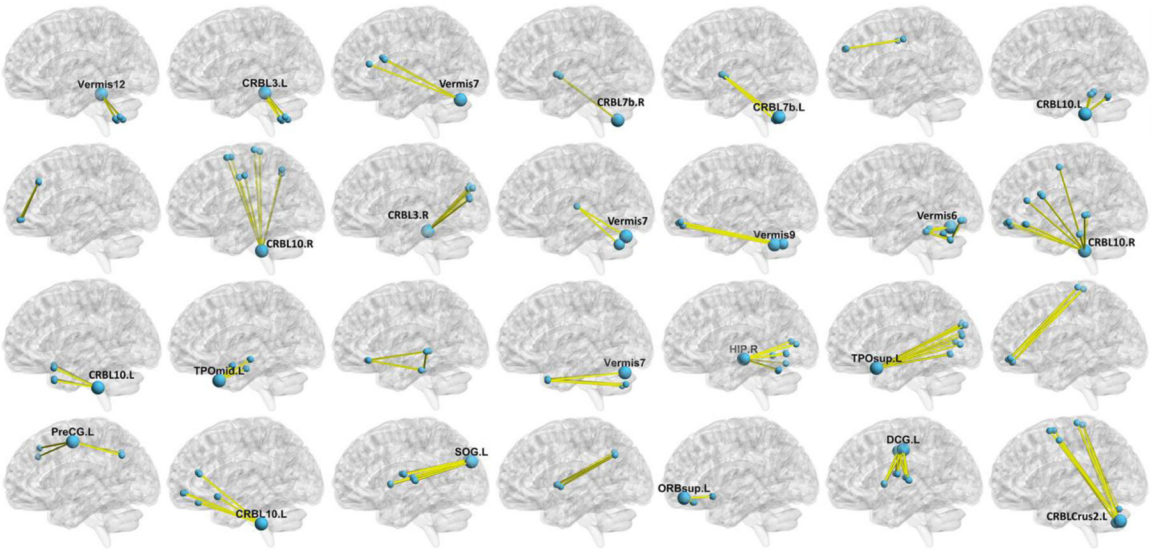

Fig. 2. The discriminative features selected based on the HON-based FED diagnosis model.

Each HON feature was represented by a group of pairwise connections in each of the subplots. The hubs (cluster centers) were highlighted with larger size (according to the nodal degree in the cluster) with their names. Abbreviations: CRBL3.L/R: left/right lobule III of cerebellar hemisphere; CRBL7b.L/R: left/right lobule VIIB of cerebellar hemisphere; CRBL10.L/R: left/right lobule X of cerebellar hemisphere; TPOmid.L: left temporal pole (middle); HIP.R: right hippocampus; TPOsup.L: left temporal pole (superior); PreCG.L: left precentral gyrus left; SOG.L: left superior occipital gyrus; ORBsup.L: left orbitofrontal cortex (superior); DCG.L: left middle cingulate gyrus; CRBLCrus2.L: left crus II of cerebellar hemisphere. More detail of each HON feature and the abbreviations of the brain regions can be found in Online Supplementary Tab. S2 and Tab. S3.

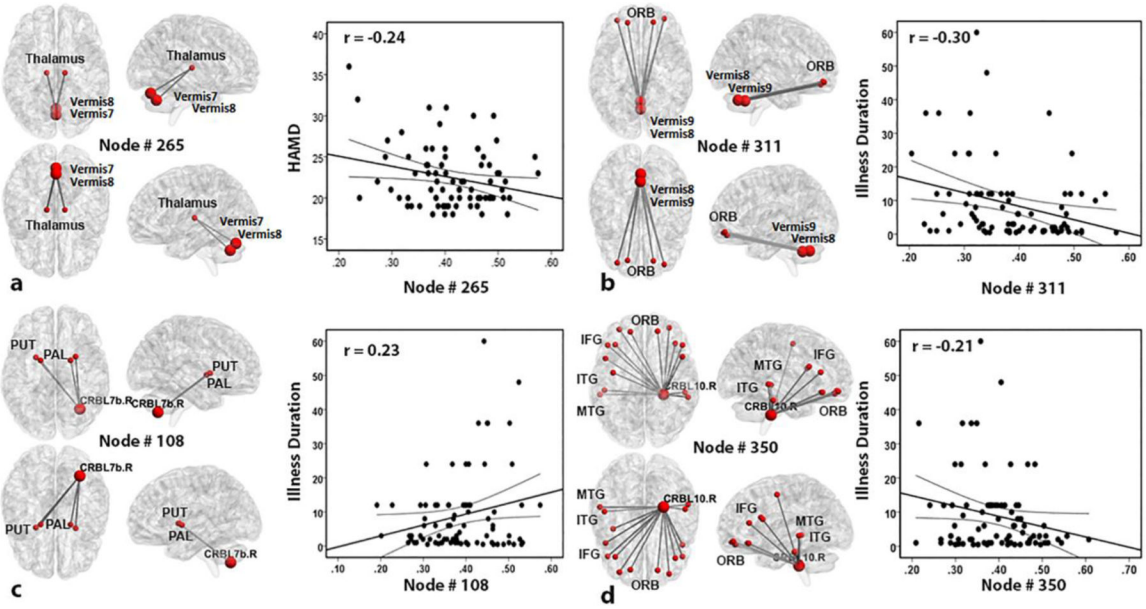

Fig. 3. Correlation between four HON features and clinical data in FED patients.

The thalamus and cerebellar vermis in HON node #265 are involved in a significant correlation between HON features and HAMD scores (**a**). Illness duration was jointly correlated with three HON features involving the HON node #311, #108 and #350, and was separately plotted with each HON node (**b-d**). Abbreviations: ORB, orbitofrontal cortex; PUT, putamen; PAL, pallidum; CRBL7b. R, right lobule VIIB of the cerebellar hemisphere; IFG, inferior frontal gyrus; MTG, middle temporal gyrus; ITG, inferior temporal gyrus; CRBL10.R, right lobule X of the cerebellar hemisphere; HAMD, 17-item Hamilton Depression Scale.

Tab. 1.

Demographic and clinical information for all subjects

	FED (N=82)	NC (N=72)	t/χ^2	*P* value
Age	30.84±10.38	29.65±10.52	0.705	0.48
Gender (M/F)	29/53	33/39	1.747	0.19
Education (yrs.)	11.77±3.48	12.43±2.48	−1.370	0.17
HAMD-17	22.46±3.72	NA	NA	NA
Illness duration (mo.)	8.96±11.64	NA	NA	NA

Abbreviations: FED, first episode depression; NC, normal control; HAMD-17, 17-item Hamilton Depression Scale; NA, not available.

Tab. 2.

Performance comparison between different methods in FED diagnosis

Method	ACC	AUC	SEN	SPE	Youden	F-score	BAC
LON	0.6753	0.7087	0.6951	0.6528	0.3479	0.6951	0.6739
HON	**0.8247**	**0.8826**	**0.8537**	**0.7917**	**0.6453**	**0.8383**	**0.8227**
HON + LON	**0.8377**	**0.9075**	**0.8415**	**0.8333**	**0.6748**	**0.8466**	**0.8374**

Abbreviations: ACC, accuracy; AUC, area under curve; SEN, sensitivity; SPE, specificity; BAC, balanced accuracy; LON, classification using LON features only (C_{LON}); HON, classification using HON features only (C_{HON}), and HON + LON, ensemble classification using both HON and LON features ($C_{HON+LON}$). The bold contents indicate the proposed methods (both C_{HON} and CHON+LON).